

# Formation time scaling and hadronization in cold nuclear matter

Alberto Accardi

*Department of Physics and Astronomy, Iowa State University,  
Ames, Iowa 50011-3160, U.S.A.*

(Dated: April 17, 2006)

I propose a scaling analysis of the hadron multiplicity ratio measured in Deep Inelastic Scattering on nuclear targets as a tool to distinguish energy loss and nuclear absorption effects on hadron suppression in cold nuclear matter. The proposed scaling variable is a function of the hadron fractional energy and of the virtual photon energy. Its functional form, which depends on a parameter  $\lambda$ , can be fixed by general theoretical considerations and encompasses both energy loss and absorption models. The parameter  $\lambda$  is fitted to HERMES experimental data and shown to favor prehadron nuclear absorption as leading mechanism for hadron suppression as opposed to quark energy loss.

PACS numbers: 25.30.-c, 25.75.-q, 24.85.+p, 13.87.Fh

## I. INTRODUCTION

[3, 4, 5, 6]

In Deep Inelastic Scattering on nuclear targets (nDIS) one observes a suppression of hadron production [1, 2, 3, 4, 5, 6, 7] analogous to hadron quenching in heavy-ion collision at the Relativistic Heavy-Ion Collider (RHIC) [8].

The cleanest environment to address nuclear modifications of hadron production is nuclear DIS: it allows to experimentally control many kinematic variables; the nuclear medium, i.e., the nucleus itself, is well known; the multiplicity in the final state is low. Moreover, the nucleons act as femtometer-scale detectors allowing to experimentally study the propagation of a parton in this “cold nuclear matter”, and its space-time evolution into the observed hadron. In the case of heavy ion collisions, one wants to use hadron suppression as a tool to extract the properties of the hot and dense system created in the collision, also called “hot nuclear matter”. If, for example, the parton’s color were neutralized on much larger scales than the nuclear radius, hadron suppression would be attributed to parton energy loss [9]. Analysis of midrapidity hadron production at RHIC in the energy loss framework leads to a medium temperature  $T \approx 400$  MeV, well in excess of the critical temperature  $T_c \approx 170$  MeV for the transition into a deconfined Quark-Gluon Plasma [10, 11]. If, on the contrary, color neutralization started on the nuclear radius scale or before, one should also account for the interactions of the medium with the prehadron, the color neutral precursor of the hadron [12]. This would lead to a different, presumably lower, value of the medium temperature. Knowing precisely how the struck quark propagates in cold nuclear matter – most importantly, whether it starts hadronizing inside or outside the nuclear medium – is essential for correctly using hadron quenching as a signature of the production of a Quark-Gluon Plasma at RHIC.

Experimental data on hadron production in nDIS are usually presented in terms of the multiplicity ratio [1, 2,

$$R_M^h(z_h, \nu) = \frac{1}{N_A^{DIS}} \frac{dN_A^h}{dz_h d\nu} \Big/ \frac{1}{N_D^{DIS}} \frac{dN_D^h}{dz_h d\nu}, \quad (1)$$

i.e., the single hadron multiplicity per DIS event on a target of mass number  $A$  normalized to the multiplicity on a deuterium target, as a function of the virtual photon energy  $\nu$  and of  $z_h = p \cdot p_h / p \cdot q$ , with  $p$  the target 4-momentum divided by  $A$ ,  $p_h$  the hadron 4-momentum and  $q$  the virtual photon 4-momentum. In the target rest frame  $z_h = E_h / \nu$  is the hadron fractional energy with respect to the virtual photon energy. The double ratios in (1) cancel to a large extent initial state effects like the modifications of parton distribution functions due to shadowing and EMC effects, exposing the nuclear modifications of the fragmentation process. If no nuclear effects modified the fragmentation process, we would expect  $R_M \approx 1$ . In fact, what is experimentally observed [1, 2, 3, 4] is a suppression of pions, kaons and antiprotons in the  $z_h = 0.1 - 1$  and  $\nu = 7 - 100$  GeV range. Protons are enhanced at  $z_h \lesssim 0.4$  (“proton anomaly”) and suppressed above. Both quenching and enhancement increase with  $A$ .

Despite a lot of experimental and theoretical efforts, the leading physical mechanism for hadron quenching in nDIS has not yet been unambiguously established. In particular, as shown in [13, 14], the observed approximate  $A^{2/3}$  scaling of the experimental data cannot distinguish models based on nuclear absorption [13, 14, 15, 16, 17] from models based on parton energy loss [11, 19], as is often assumed. Indeed, single hadron suppression in nDIS obeys a  $A^{2/3}$  law (broken at  $A \gtrsim 80$ ) in both energy loss and absorption models [13]. Even the more refined analysis in terms of  $R_M = cA^\alpha$  fits proposed in [14] cannot clearly distinguish the 2 classes of models.

In this paper, I propose a scaling analysis of  $R_M$  as a tool to disentangle parton energy loss and nuclear absorption effects on hadron production in nDIS. More in detail, I conjecture that  $R_M$  should not depend on  $z_h$  and  $\nu$  separately but should depend on a combination of

them:

$$R_M = R_M [\tau(z_h, \nu)] , \quad (2)$$

where the scaling variable  $\tau$  is defined as

$$\tau = C z_h^\lambda (1 - z_h) \nu . \quad (3)$$

The scaling exponent  $\lambda$  is introduced as a way of approximating and summarizing the scaling behavior of experimental data and theoretical models. It will be separately obtained by a best fit analysis of data and theoretical computations, see Section III. The proportionality constant  $C$  cannot be determined by the fit. A possible scaling of  $R_M$  with  $Q^2$  is not considered in this analysis because of its model dependence; moreover, in the HERMES data considered in this paper, the dependence of the average  $\langle Q^2 \rangle$  on  $z_h$  and  $\nu$  is very mild, implying very small effects on the scaling of  $R_M$ .

As discussed in Section II, the proposed functional form of  $\tau$  is flexible enough to encompass both absorption models and energy loss models. The 2 classes of models are distinguished by the value of the scaling exponent: a positive  $\lambda \gtrless 0$  is characteristic of absorption models, while a negative  $\lambda \lesssim 0$  is characteristic of energy loss models. Thus, the exponent  $\lambda$  obtained in the proposed model-independent scaling analysis of experimental data can identify the leading mechanism for hadron suppression in nDIS.

## II. SCALING OF $R_M$

The idea that the hadron multiplicity ratio  $R_M$  should scale with the variable  $\tau$  introduced in Eq. (3) is quite natural in the context of hadron absorption models [14, 15, 16, 17]. In these models the struck quark neutralizes its color on a relative short time scale. The ensuing color neutral state, called a prehadron, later on collapses on the wave function of the observed hadron. Hadron suppression is then mainly attributed to prehadron-nucleons interactions, whose magnitude depends on the in-medium prehadron path length, which depends solely on the prehadron formation time  $t_*$ .

Estimates of the prehadron formation time can be obtained in the framework of the Lund string model [14, 15, 18], where the prehadrons are identified with each of the fragments of the color string. Alternatively, in the pQCD inspired color dipole model for leading hadron suppression of Ref. [16], the hardest gluon radiated off the struck quark splits into a quark-antiquark pair; the antiquark then recombines with the struck quark into the leading prehadron. In both cases the prehadron formation time has a simple general form:

$$t_* = g(z_h)(1 - z_h) \frac{\nu}{\kappa} , \quad (4)$$

where  $g(z_h) \rightarrow 0$  as  $z_h \rightarrow 0$ , and  $\kappa$  is a constant that sets the time scale of hadronization. In the Lund model  $\kappa \approx 1$

GeV/fm is given by the string tension; in the dipole model  $\kappa = Q^2$ . At HERMES, in both models, the prehadron formation time is  $t_* \lesssim 5$  fm, which is smaller than the nuclear radius. On the contrary, hadrons are typically produced at the periphery or outside the target nucleus and their absorption does not contribute much to  $R_M$ . The physical origin of  $t_*$  is transparent. The factor  $\nu$  can be understood as a Lorentz boost factor. At large  $z_h$  the hadron carries away most of the struck quark energy. The color string remainder has only an energy  $(1 - z_h)\nu$  left, so that it cannot stretch farther off (in pQCD terms, the colored struck quark has a little energy to radiate into gluons, hence it must neutralize its color in a short time). At small  $z_h \rightarrow 0$  the prehadron formation time should go to 0, as well, as explicitly shown in Lund model computations [14, 15, 18]. This follows from the fact that we are discussing semi-inclusive hadron measurements. At small  $z_h$  the observed hadron carries away a small fraction of the struck quark energy. The rest of the energy will most probably be used for the creation of other low energy prehadrons, because the string fragmentation function is steeply falling with  $z_h$ . On average, the observed prehadron will be produced close to the interaction point.

Summarizing the above discussion,  $R_M$  in absorption models should depend only on  $t_* = t_*(z_h, \nu)$  and not on  $z_h$  and  $\nu$  separately. A good approximation to  $t_*$  is the scaling variable  $\tau$  of Eq. (3), where the scaling exponent  $\lambda$  depends on the chosen absorption model. A rough estimate of the scaling exponent gives  $\lambda \approx 1$ . A more precise value can be obtained by fitting Eqs. (2)-(3) to the theory model results [13, 14, 16, 17] for  $R_M$ . The fit procedure, explained in detail in the next section, results in  $0.5 \lesssim \lambda \lesssim 1.2$  for absorption models.

In energy loss models [11, 19] the hadron formation time is assumed to be much larger than the nuclear radius, and the hadronization process is assumed to happen entirely outside the target nucleus. The quark travels through the nucleus and experiences multiple scatterings and induced gluon bremsstrahlung. Hence, it starts the hadronization process with a reduced energy  $\nu - \epsilon$  where  $\epsilon$  is the energy of the radiated gluons.

In Ref. [19], extended in [13] to include finite medium size corrections, the reduced quark energy at the time of hadronization is translated in a shift of  $z_h$  in the vacuum fragmentation function  $D$  [20]. The medium modified FF is then computed as

$$\tilde{D}_A(z_h) = \int_0^{(1-z_h)\nu} d\epsilon \mathcal{P}(\epsilon) \frac{1}{1 - \epsilon/\nu} D\left(\frac{z_h}{1 - \epsilon/\nu}\right) , \quad (5)$$

where the dependence of the vacuum FF on the hard scale scale  $Q^2$  of the process is understood, and the quenching weight  $\mathcal{P}(\epsilon)$  is the probability distribution of an energy loss  $\epsilon$  computed in the Baier-Dokshitzer-Mueller-Schiff formalism [21]. Note the upper limit of integration in Eq. (5) imposed by energy conservation. For the purpose of discussing the scaling properties of  $R_M$ , we can work in the soft gluon approximation, and neglect finite

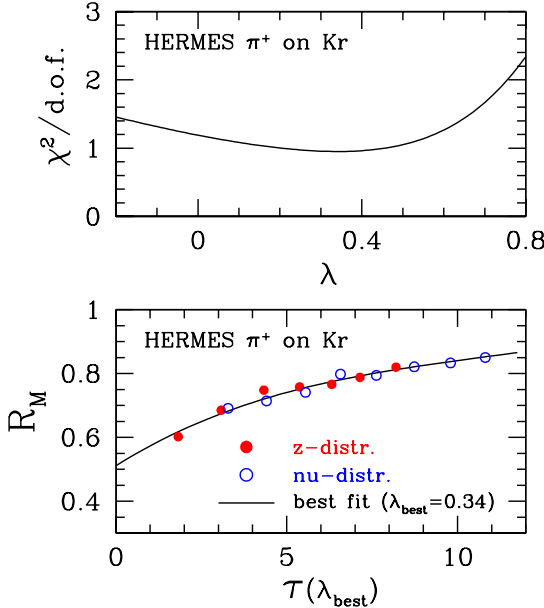


FIG. 1: An example of the fit procedure described in Section 3, applied to  $\pi^+$  production on a Kr target at HERMES [3]. Upper panel:  $\chi^2/\text{d.o.f.}$  as a function of  $\lambda$ . Lower panel:  $R_M(\tau)$  with  $\tau$  computed at  $\lambda_{\text{best}} = 0.34$ . Experimental statistical errors are of the same size as the plotted points.

quark energy corrections, which would introduce an additional  $\nu$  dependence in the quenching weight [22]. If we further neglect energy loss fluctuations, we can approximate  $R_M \approx \tilde{D}_A(z_h)/D(z_h)$  and obtain

$$R_M \approx \frac{1}{1 - \langle \epsilon \rangle / \nu} D \left( \frac{z_h}{1 - \langle \epsilon \rangle / \nu} \right) [D(z_h)]^{-1}, \quad (6)$$

where the average energy loss  $\langle \epsilon \rangle = \int_0^{(1-z_h)\nu} d\epsilon \epsilon \mathcal{P}(\epsilon) = f[(1-z_h)\nu]$  is a function of the energy  $(1-z_h)\nu$  not carried away by the observed hadron. Next, we can approximate the FF using the parametrization of Ref. [23] at  $Q^2 = 2 \text{ GeV}^2$ :  $D(z_h) = C z_h^\alpha (1-z_h)^\beta$ , where for pions  $\alpha \approx -1$ ,  $\beta \approx 1.5$  and the constant  $C$  will cancel in the multiplicity ratio. Finally,

$$R_M \approx \frac{1}{\left(1 - \frac{1}{\nu} f[(1-z_h)\nu]\right)^{\alpha+\beta+1}} \left(1 - \frac{f[(1-z_h)\nu]}{(1-z_h)\nu}\right)^\beta \quad (7)$$

which shows an approximate scaling with  $(1-z_h)\nu$ .

In Ref. [11] the medium modifications of the fragmentation functions are computed from twist-4 contributions to the leading order cross-section, including diagrams with one elastic quark-nucleus scattering and one radiated gluon. Both the struck quark and the radiated gluon are allowed to fragment according to vacuum FF. The obtained modified FF,  $\tilde{D}$ , can be well approximated by the numerator in Eq. (6) with  $\epsilon/\nu = 0.6 \langle z_g \rangle$ , where  $\langle z_g \rangle$  is the

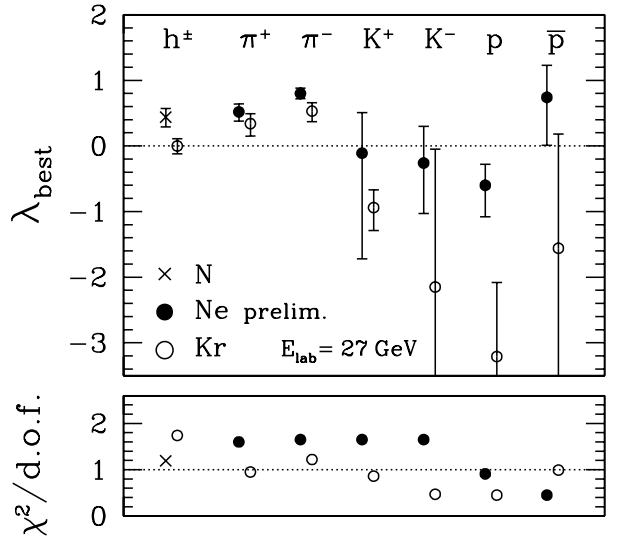


FIG. 2: The scaling exponent  $\lambda_{\text{best}}$  extracted from HERMES data on charged and identified hadrons at  $E_{\text{lab}} = 27 \text{ GeV}$  [2, 3, 4] (only statistical errors included in the fit). Error bars correspond to 1 standard deviation. The bottom panel shows the  $\chi^2$  per degree of freedom.

average fractional energy of the radiated gluon [11, 24]:

$$\begin{aligned} \langle z_g \rangle &= \int_0^{\mu^2} \frac{d\ell_T^2}{\ell_T^2} \int_0^{1-z_h} dz_g \frac{\alpha_s}{2\pi} z_g \Delta \gamma_{q \rightarrow gq}(z_g, \ell_T^2) \\ &\approx \alpha_s^2(Q^2) \tilde{C}(Q^2) m_N R_A^2 \frac{1}{\nu} f_g(1-z_h) \\ &\equiv \frac{k}{0.6} \frac{1}{\nu} f_g(1-z_h). \end{aligned} \quad (8)$$

Here,  $\gamma_{q \rightarrow gq}$  is the quark-gluon splitting function,  $\tilde{C}(Q^2)$  is the strength of parton-parton correlations in the nucleus,  $m_N$  the nucleon mass,  $R_A$  the nuclear radius, and  $k$  is a shorthand for the quantities independent of  $z_h$  and  $\nu$ .  $f_g$  is a function of  $1-z_h$  because of the upper limit of integration on  $z_g$  imposed by energy conservation. In the HERMES regime,  $f_g(1-z_h) \propto (1-z_h)^{0.4}$ . Approximating  $R_M$  and the modified FF as before we have:

$$R_M \approx \frac{1}{\left(1 - \frac{k}{\nu} f_g(1-z_h)\right)^{\alpha+\beta+1}} \left(1 - \frac{k f_g(1-z_h)}{(1-z_h)\nu}\right)^\beta. \quad (9)$$

From Eqs. (7) and (9) a scaling of  $R_M$  with  $(1-z_h)$  is evident, which implies  $\lambda = 0$  in Eq. (3). However, it is not immediate to see the role played by  $\nu$ . To establish it, let's introduce an effective scaling variable  $\tau' = C z_h^\lambda (1-z_h) \nu^\mu$ , with  $\mu$  an effective parameter describing the scaling of  $R_M$  with respect to  $\nu$  in energy loss models. The value of  $\mu$  can be determined by a fit of the full computations in Refs. [11, 13] as follows. For any given  $\mu$ , we fit the theoretical  $R_M = R_M(\tau')$  and determine  $\lambda = \lambda(\mu)$  by  $\chi^2$  minimization as described in Section III. A scaling of  $R_M$  with  $\tau'$  (i.e.,  $\chi^2/\text{d.o.f.} < 1$ )

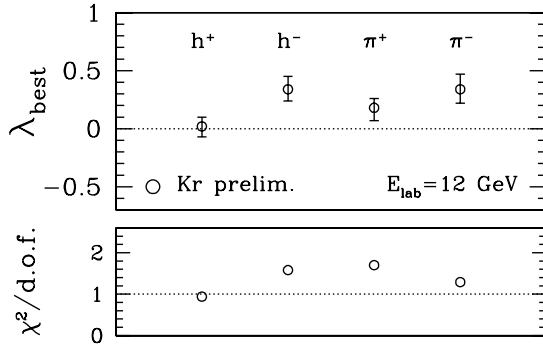


FIG. 3: The scaling exponent  $\lambda_{\text{best}}$  for HERMES data at  $E_{\text{lab}} = 12$  GeV on a Kr target [5]. The N target results are not shown because of their very large error bars. The bottom panel shows the  $\chi^2$  per degree of freedom.

is found for  $0.2 \lesssim \mu \lesssim 1.8$ , with the best-fit  $\lambda$  decreasing as  $\mu$  increases. As expected on theoretical grounds, in this range of  $\mu$  values  $\lambda_{\text{best}} \lesssim 0$ , which distinguishes it from the positive  $\lambda$  expected in absorption models.

In conclusion, for the sake of comparing energy loss models with absorption models and without loss of generality, we can fix  $\mu = 1$  and analyze experimental data and theory models in terms of the proposed scaling variable  $\tau$  in Eq. (3).

### III. FIT PROCEDURE AND RESULTS

The HERMES experiment measures  $R_M$  binned in  $z_h$  and integrated over  $\nu$  and  $Q^2$  (“ $z_h$  distributions”) or binned in  $\nu$  and integrated over  $z_h$  and  $Q^2$  (“ $\nu$  distributions”). The scaling of experimental data with respect to the variable  $\tau$  defined in Eq. (3) and the scaling exponent  $\lambda$  can be determined by a fit to the data as follows.

- (1) Fix  $\lambda$ .
- (2) For each  $z_h$  bin in  $z_h$ -distributions compute  $\tau = \tau(z_h, \langle \nu(z_h) \rangle)$  and  $R_M(\tau) \equiv R_M(z_h)$ , where  $\langle \nu(z_h) \rangle$  is the average measured  $\nu$  in the considered  $z_h$ -bin. Likewise for each  $\nu$  bin in  $\nu$ -distributions compute  $\tau = \tau(\langle z_h(\nu) \rangle, \nu)$  and  $R_M(\tau) \equiv R_M(\nu)$ .
- (3) Fit a function  $\phi(\tau)$  to the pairs  $\{(\tau, R_M)\}$  obtained at step 2, and compute  $\chi^2 = \chi^2(\lambda)$ . The choice of  $\phi$  is discussed below.
- (4) Determine the best-fit exponent  $\lambda_{\text{best}}$  by minimization of  $\chi^2(\lambda)$ .
- (5) If  $\chi^2(\lambda_{\text{best}}) \lesssim 1$  per degree of freedom, we say that the analyzed data set scales with respect to the  $\tau$  variable, and is characterized by a scaling exponent  $\lambda_{\text{best}}$ .

An example of this procedure and the corresponding  $R_M(\tau)$  computed at  $\lambda = \lambda_{\text{best}}$  is illustrated in Fig. 1. The

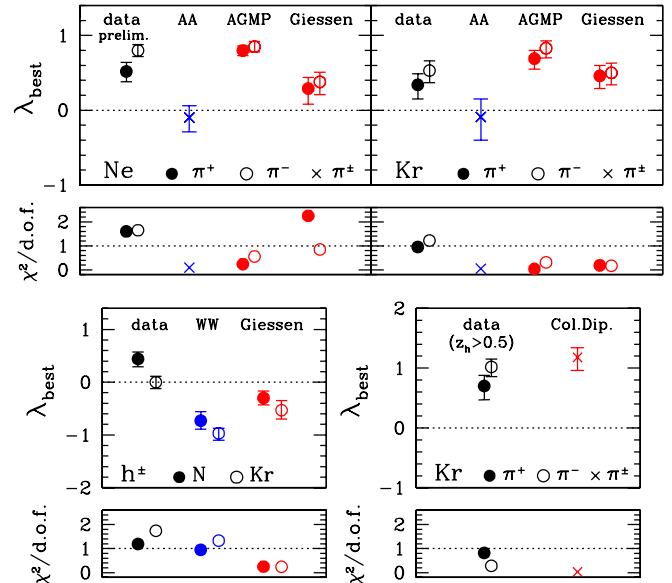


FIG. 4: Comparison of the scaling exponent for  $\pi^\pm$  and  $h^\pm$  from HERMES data at  $E_{\text{lab}} = 27$  GeV [2, 3, 4] and from theory models. Error bars correspond to 1 standard deviation. Energy loss models (blue points on-line): AA [13], WW [11]. Absorption models (red points): AGMP (pure absorption without  $Q^2$ -rescaling) [13, 14], Col.Dip. [16]. The Giessen model [17] embeds nuclear absorption in a full Monte Carlo simulation of the nDIS event. The bottom panels show the  $\chi^2$  per degree of freedom.

fit to theoretical computations is done in the same way as the fit to HERMES data, by considering the computed  $R_M$  at the central value of each  $z_h$  and  $\nu$  experimental bin. Theoretical errors are estimated as 6% of  $1 - R_M$  for the models of Refs. [11, 13, 14, 17], which need to fit 1 parameter to  $R_M$  data [14], and 10% for the model of Ref. [16].

The fit results discussed below have been obtained using as fit function  $\phi(\tau)$  a polynomial of 4<sup>th</sup> degree in  $\tau$ . The results of the fit have been cross-checked by using a rational function of second order constrained to tend to 1 as  $\tau \rightarrow \infty$ , which has 5 free parameters as the default polynomial. A second cross-check was obtained by additionally constraining the rational function to have null derivative at  $\tau = 0$  in order to avoid singularities. Finally, unless otherwise explicitly stated, for this scaling analysis I considered only data points satisfying the following cuts: (i)  $z_h > 0.2$ , to avoid the target fragmentation region, for which the conjectured scaling is not valid, and to avoid large corrections due to the detector geometric acceptance [17]; (ii)  $z_h < 0.9$ , to avoid diffractive hadron production and quasi-elastic lepton-nucleon scatterings; (iii)  $\nu > 7$  GeV, for consistency between the analysis of the N, Kr and Ne target data sets. For each target and hadron flavor 14 data points survive these cuts.

The scaling exponents  $\lambda_{\text{best}}$  extracted from HERMES data at  $E_{\text{lab}} = 27$  GeV [2, 3, 4] and 12 GeV [5] for differ-

ent hadron flavors produced on N, Ne and Kr targets are shown in Fig. 2. In all cases  $\chi^2/\text{d.o.f.} \lesssim 1.6$ , which proves that  $R_M$  scales with  $\tau$ . The central result of this paper is that pion data exhibit a clear  $\lambda_{\text{best}} \approx 0.4 \gtrless 0$ . As discussed in the previous section, this shows in a model independent way the dominance of the prehadron absorption mechanism as opposed to the energy loss mechanism. This conclusion is confirmed by the comparison to theory models shown in Fig. 4.

Unidentified charged hadrons ( $h^\pm$ ) have a positive  $\lambda_{\text{best}}$  on N target, but  $\lambda_{\text{best}} \approx 0$  on Kr target. This apparently contradictory result can be explained in terms of the proton contribution to the  $h^\pm$  sample. Proton production shows an anomalous enhancement of  $R_M$  above 1 when  $z_h \lesssim 0.4$ , which cannot be explained in terms of either parton energy loss or prehadron absorption, and is not yet fully understood theoretically. The proton anomaly explains the negative value of its scaling exponent  $\lambda_{\text{best}}$ , which in turn drives the  $h^\pm$  value of  $\lambda_{\text{best}}$  towards 0 for heavy targets. Indeed, by cutting the  $h^\pm$  sample on Kr target at  $z_h > 0.5$  one obtains a reduced  $\chi^2/\text{d.o.f.} = 1.18$  and  $\lambda_{\text{best}} = 0.34 \pm 0.13$ , compatible with the  $\pi^\pm$  exponents and the nuclear absorption mechanism. A further confirmation of the role of proton anomaly in reducing the scaling exponent comes from preliminary data on Kr at  $E_{\text{lab}} = 12$  GeV [5], which yield  $\lambda_{\text{best}} = 0.02 \pm 0.09$  for  $h^+$  and  $\lambda_{\text{best}} = 0.34 \pm 0.11$  for  $h^-$ , see Fig. 3.

From kaons and antiprotons data it is difficult to draw any conclusion because of the large error bars.

#### IV. SUMMARY AND CONCLUSIONS

In this work, I proposed a scaling analysis of hadron attenuation in nDIS as a tool to investigate quark

hadronization in cold nuclear matter, and to distinguish parton energy loss from nuclear absorption effects in the experimental data. The scaling properties of experimental data and theory computations of the hadron attenuation ratio  $R_M$  can be summarized by the value of the exponent  $\lambda$  in the scaling variable  $\tau$  introduced in Eq. (3). The exponent  $\lambda$  is able to clearly distinguish models based on parton energy loss ( $\lambda \lesssim 0$ ) from models based on hadron absorption ( $\lambda \gtrsim 0.5$ ). Experimental data on pion and charged hadron production have been shown to scale with  $\tau$  and exhibit  $\lambda \approx 0.4 \pm 0.1$ , which is a clear indication that the hadronization process starts on a time scale of the order of a few Fermi, and that prehadron nuclear absorption dominates hadron quenching in nuclear DIS. The scaling variable  $\tau$  can then be interpreted as a measure of the formation time of the prehadron, the color neutral precursor of the observed hadron. An independent test of these conclusions, and a measure of the overall normalization of the prehadron formation time  $\tau$ , can be obtained considering more exclusive observable, like the  $z_h$ -dependence of hadron's  $p_T$ -broadening and Cronin effect [16]. Establishing a scaling of the prehadron formation time with  $Q^2$ , as predicted, e.g., in Ref. [16], will further constrain the hadronization mechanism. A dedicated experimental analysis is needed to improve the reach and precision of the scaling analysis presented in this paper.

**Acknowledgments.** I am grateful to P. Di Nezza, V. Muccifora and J.W. Qiu for valuable discussions and their support; to F. Arleo, T. Falter and K. Gallmeister for detailed discussions on their models; to INFN Frascati and INFN Milan for hospitality during the preparation of this work. This work is partially funded by the US Department of Energy grant DE-FG02-87ER40371.

---

[1] J. Ashman *et al.* [EMC], Z. Phys. C **52** (1991) 1.  
[2] A. Airapetian *et al.* [HERMES], Eur. Phys. J. C **20** (2001) 479.  
[3] A. Airapetian *et al.* [HERMES], Phys. Lett. B **577** (2003) 37;  
[4] G. Elbakian [HERMES], Proceedings of “DIS 2003”, St.Petersburg, April 23-27, 2003; V.T. Kim and L.N. Lipatov eds., page 597.  
[5] P. B. van der Nat [HERMES], <http://www-hermes.desy.de/notes/pub/trans-public-subject.html>  
[6] B. A. Mecking *et al.* [CLAS], Nucl. Instrum. Meth. A **503** (2003) 513; W. K. Brooks, FizikaB **13** (2004) 321 and talk at “Parton Propagation through Strongly Interacting Matter”, 27 Sep - 7 Oct 2005, ECT\*, Trento (ITA).  
[7] A. Airapetian *et al.* [HERMES], Phys. Rev. Lett. (in press) [arXiv:hep-ex/0510030].  
[8] I. Arsene *et al.* [BRAHMS], Nucl. Phys. A **757**, 1 (2005); B. B. Back *et al.* [PHOBOS], Nucl. Phys. A **757**, 28 (2005); J. Adams *et al.* [STAR], Nucl. Phys. A **757**, 102 (2005); K. Adcox *et al.* [PHENIX], Nucl. Phys. A **757** (2005) 184.  
[9] M. Gyulassy, I. Vitev, X. N. Wang and B. W. Zhang, in “Quark Gluon Plasma 3”, R.C. Hwa and X.N. Wang eds., World Scientific, Singapore [arXiv:nucl-th/0302077].  
[10] I. Vitev, J. Phys. G **30** (2004) S791.  
[11] E. Wang and X. N. Wang, Phys. Rev. Lett. **89** (2002) 162301.  
[12] W. Cassing, K. Gallmeister and C. Greiner, Nucl. Phys. A **735** (2004) 277.  
[13] A. Accardi, arXiv:nucl-th/0510090.  
[14] A. Accardi, D. Grunewald, V. Muccifora and H. J. Pirner, Nucl. Phys. A **761** (2005) 67.  
[15] A. Accardi, V. Muccifora and H. J. Pirner, Nucl. Phys. A **720**, 131 (2003).  
[16] B. Z. Kopeliovich, J. Nemchik, E. Predazzi and A. Hayashigaki, Nucl. Phys. A **740** (2004) 211.  
[17] T. Falter, W. Cassing, K. Gallmeister and U. Mosel, Phys. Rev. C **70** (2004) 054609.  
[18] A. Bialas and M. Gyulassy, Nucl. Phys. B **291** (1987)

793.

- [19] F. Arleo, Eur. Phys. J. C **30** (2003) 213.
- [20] X. N. Wang, Z. Huang and I. Sarcevic, Phys. Rev. Lett. **77** (1996) 231.
- [21] R. Baier, Y. L. Dokshitzer, A. H. Mueller and D. Schiff, JHEP **0109**, 033 (2001) ; C. A. Salgado and U. A. Wiedemann, Phys. Rev. D **68** (2003) 014008.
- [22] F. Arleo, JHEP **0211** (2002) 044.
- [23] B. A. Kniehl, G. Kramer and B. Potter, Nucl. Phys. B **582** (2000) 514.
- [24] X. N. Wang and X. f. Guo, Nucl. Phys. A **696** (2001) 788 and Phys. Rev. Lett. **85** (2000) 3591.